

# Elucidating the lack of magnetic order in the heavy fermion CeCu<sub>2</sub>Mg

H. Michor<sup>1</sup>, J.G. Sereni<sup>2</sup>, M. Giovannini<sup>3</sup>, E. Kampert<sup>4</sup>, L. Salamakha<sup>1</sup>, G. Hilscher<sup>1†</sup>, E. Bauer<sup>1</sup>

<sup>1</sup>*Institute of Solid State Physics, TU Wien, A-1040 Wien, Austria*

<sup>2</sup>*Low Temperature Division CAB-CNEA, CONICET, 8400 S.C. de Bariloche, Argentina*

<sup>3</sup>*Dipartimento di Chimica e Chimica Industriale, Università di Genova, I-16146 Genova, Italy  
and CNR-SPIN Corso Perrone, I-16152 Genova, Italy*

<sup>4</sup>*Dresden High Magnetic Field Laboratory, Helmholtz-Zentrum Dresden-Rossendorf, D-01314 Dresden, Germany*

Magnetic, transport, and thermal properties of CeCu<sub>2</sub>Mg are investigated to elucidate the lack of magnetic order in this heavy fermion compound with a specific heat value,  $C_{\text{mag}}/T|_{T \rightarrow 0} \approx 1.2 \text{ J/molK}^2$  and robust effective magnetic moments ( $\mu_{\text{eff}} \approx 2.46 \mu_{\text{B}}$ ). The lack of magnetic order is attributed to magnetic frustration favored by the hexagonal configuration of the Ce sub-lattice. In fact, the effect of magnetic field on  $C_{\text{mag}}/T$  and residual resistivity  $\rho_0$  does not correspond to that of a Fermi-liquid (FL) because a broad anomaly appears at  $T_{\text{max}} \approx 1.2 \text{ K}$  in  $C_{\text{mag}}(T)/T$ , without changing its position up to  $\mu_0 H = 7.5 \text{ T}$ . However, the flattening of  $C_{\text{mag}}/T|_{T \rightarrow 0}$  and its magnetic susceptibility  $\chi_{T \rightarrow 0}$ , together with the  $T^2$  dependence of  $\rho(T)$ , reveal a FL behavior for  $T \leq 2 \text{ K}$  which is also supported by Wilson and Kadowaki-Woods ratios. The unusual coexistence of FL and frustration phenomena can be understood by placing paramagnetic CeCu<sub>2</sub>Mg in an intermediate section of a frustration-Kondo model. The entropy,  $S_{\text{mag}}$ , reaches  $0.87 R \ln 6$  at  $T \simeq 100 \text{ K}$ , with a tendency to approach the expected value  $S_{\text{mag}} = R \ln 6$  of the  $J = 5/2$  ground state of Ce<sup>3+</sup>.<sup>a</sup>

## I. INTRODUCTION

Heavy fermions are characterized by a high density of low energy excitations that increases by lowering the temperature. This scenario is induced by the hybridization ( $\Gamma_{sf}$ ) of the localized  $4f$  and conduction states [1], producing a progressive screening of the  $4f$  magnetic moments as the temperature drops below a characteristic (Kondo) temperature,  $T_K \propto \Gamma_{sf}$ . For large  $T_K$  values (strong hybridization) magnetism is suppressed because magnetic moments are fully screened by conduction electron spins and the system behaves as a Fermi liquid (FL), where the Sommerfeld coefficient of the specific heat  $\gamma = C_{\text{mag}}/T \propto m_{\text{eff}}$ , with  $C_{\text{mag}}$  being the magnetic contribution to specific heat and  $m_{\text{eff}}$  the effective mass of FL quasi-particles. For intermediate  $T_K$  (moderate  $\Gamma_{sf}$ ), the ground state (GS) degrees of freedom progressively accumulate at low energy, with a consequent growing of the density of states reflected in the  $\gamma$  enhancement.

Upon a further decrease of  $T_K$ ,  $C_{\text{mag}}/T \equiv \gamma_T$  becomes temperature dependent at  $T \rightarrow 0$ . In this non-Fermi liquid regime, a typical  $C_{\text{mag}}(T)/T \propto -\ln(T/T_0)$  dependence is observed [2], where  $T_0$  represents an energy scale similar to  $T_K$  for FL systems. Depending on the number of electrons in the conduction band, the electronic spins may or not be able to fully screen the localized magnetic moments. In the so called under-screened regime [3], the system may order magnetically (at  $T_{\text{ord}}$ ), with a fraction of the total GS degrees of freedom (usually  $R \ln 2$ ) condensed into the ordered phase when  $T_{\text{ord}} \approx T_K$ .

In the Doniach-Lavagna [4, 5] model, the competition between  $T_{\text{ord}}$  and  $T_K$  depends on the ratio of the respective coupling parameters  $J_{\text{ord}}$  and  $J_K$ . For low values, the system is expected to order magnetically because  $T_{\text{ord}} \propto J_{\text{ord}}^2$  grows faster than  $T_K \propto \exp[-1/n(E_F)J_K]$  where  $n(E_F)$  is the electronic density of states at the Fermi level. There is, however, an increasing number of Ce and Yb based compounds that do not order magnetically despite of their robust magnetic moments, i.e. possessing low  $T_K$  values [6]. This is the case of ternary CeCu<sub>2</sub>Mg crystallizing in the GdPt<sub>2</sub>Sn type structure [7].

Different origins can be argued for such anomalous behavior: i) dilute or disordered magnetic moments, ii) large interatomic distance between magnetic atoms, iii) weak exchange interaction  $J_{\text{ord}}$  or iv) frustrated magnetic interactions. Alternative i) does not apply to a Ce-lattice compound neither ii) because in CeCu<sub>2</sub>Mg the Ce-Ce distance lies within the range of many ordered compounds [8].

With the aim to verify the lack of magnetic order below  $T = 1.5 \text{ K}$  and to elucidate the nature of the GS of this compound, magnetic and thermal properties are newly studied in this work extending the range of measurements down to  $T \approx 0.5 \text{ K}$ .

## II. EXPERIMENTAL DETAILS

The samples were prepared using cerium 99.9 mass %, magnesium and copper 99.99 mass % supplied by Newmet Koch, Waltham Abbey, England as starting materials. The samples were prepared by induction melting stoichiometric amounts of the elements enclosed in a small arc-sealed tantalum crucibles. The alloys were then annealed at  $500^\circ\text{C}$  for 20 days and characterized by electron probe micro-analysis (EPMA) and X-ray powder diffraction (XRD).

<sup>a</sup> ©2017 APS. This is the peer reviewed version of the following article: Michor, H., Sereni, J.G., Giovannini, M., Kampert, E., Salamakha, L., Hilscher, G., Bauer, E., Elucidating the lack of magnetic order in the heavy fermion CeCu<sub>2</sub>Mg, Physical Review B **95**, 115146-1-7 (2017) which has been published in final form at <https://doi.org/10.1103/PhysRevB.95.115146>.

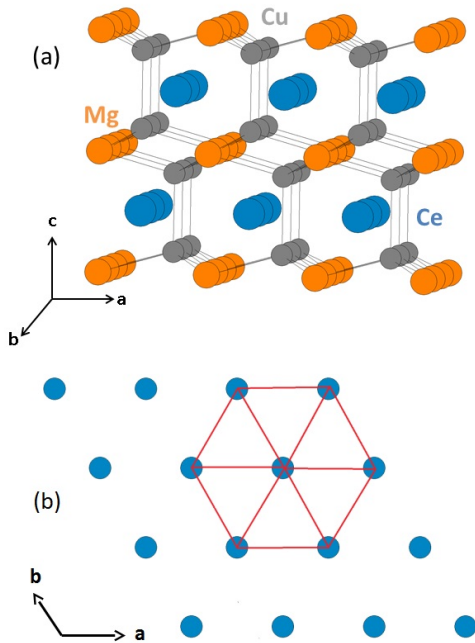


FIG. 1. (Color online) (a) Crystal structure of CeCu<sub>2</sub>Mg. Cerium (blu), copper (gray) magnesium (orange). (b) Ce-layers in the 'ab' plane. The hexagonal lattice of Ce atoms is sketched for a Ce atom having six first neighbors.

Magnetization was measured employing a CRYOGENIC S700X superconducting quantum interference device (SQUID) magnetometer at temperatures from 0.3 to 2 K with a <sup>3</sup>He-insert and from 1.8 K to room temperature with standard <sup>4</sup>He variable temperature insert. An additional high-field magnetization measurement at 1.6 K and at fields up to 60 T was performed at the Dresden High Magnetic Field Laboratory using a pulse field system with a 1.44 MJ capacitor module (see Ref. [9] for further details).

Low temperature specific heat data were measured using various setups: (i) with a standard heat pulse technique in a semi-adiabatic He-3 calorimeter in the range between 0.5 and 7 K, at zero and applied magnetic field up to 4 T, (ii) with a Quantum Design PPMS relaxation-type calorimeter with <sup>3</sup>He-insert between 0.5 and 10 K in magnetic fields up to 7.5 T, (iii) with PPMS <sup>4</sup>He specific heat puck in zero-field and a temperature range of 2 to 120 K.

The electrical resistivity and magneto-resistivity of bar shaped samples (about 0.5 × 0.5 × 3 mm<sup>3</sup>) were measured using a four-probe ac bridge method with spot-welded gold contacts in the temperature range from 0.4 K to 25 K and in magnetic fields up to 12 T.

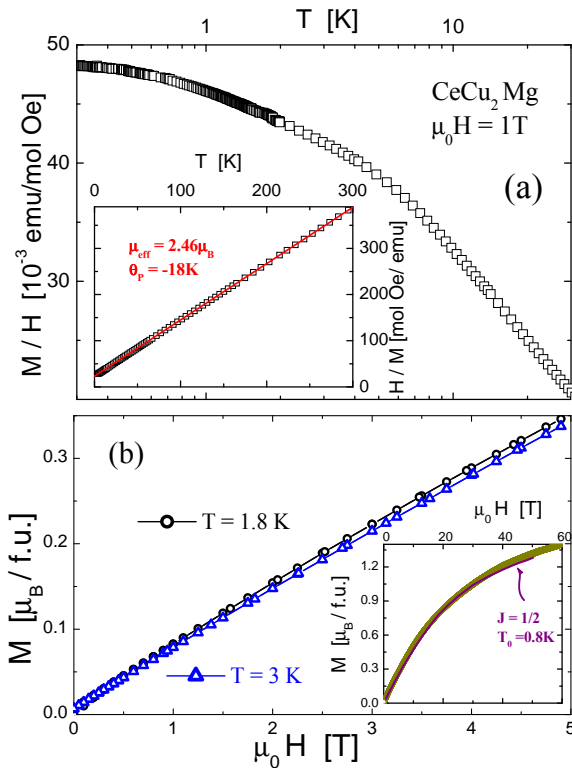


FIG. 2. (Color online) (a) Low temperature ( $T < 25$  K) thermal dependence of the magnetic susceptibility in a semi-logarithmic representation. Inset: Temperature dependent inverse magnetic susceptibility, with a Curie-Weiss fit, Eqn. (1), shown as solid line. (b) Field dependent isothermal magnetization at temperatures as labeled. Inset: High field magnetization data measured up to 60 T at 1.6 K.

### III. EXPERIMENTAL RESULTS

#### A. Structural properties

A refinement of X-ray patterns for CeCu<sub>2</sub>Mg [7] confirmed that this compound crystallizes in the hexagonal GdPt<sub>2</sub>Sn structure type (space group  $P6_3/mmc$ ), named also as ZrPt<sub>2</sub>Al- or LiCu<sub>2</sub>Sn- type [10]. The lattice parameters are  $a = 4.657$  Å and  $c = 8.654$  Å. In this hexagonal structure constituent atoms are stacked in layers perpendicular to the  $c$  axis in regular sequences of Mg, Cu, Ce, and Cu as shown in Fig. 1a. In the Ce-layers atoms are well separated from each other, forming a hexagonal lattice (shown in Fig. 1b) where Ce atoms have six first neighbors placed at the Ce-Ce shortest distances corresponding to the lattice parameter  $a$ . Moreover, Ce atoms fill large highly symmetric rhombic dodecahedron cages of coordination number 14 (8 Cu + 6 Mg).

## B. Magnetic Properties

The low temperature ( $T < 25$  K) thermal dependence of the magnetic susceptibility (defined as  $\chi = M/H$ ) is shown in Fig. 2a in a semi-logarithmic representation. Below about 10 K  $\chi(T)$  tends to flatten due to an antiferromagnetic interaction, which leads to a negative paramagnetic Curie temperature  $\theta_p = -18$  K [7]. Above 10 K, the usual  $\chi \propto 1/T$  dependence is recovered (see the inset of Fig. 2a). The experimental results are properly described by a classical Curie-Weiss law, including a moderate Pauli like contribution ( $\chi_0$ ):

$$\chi = C/(T + \theta_p) + \chi_0, \quad (1)$$

with the Curie constant  $C = N_A \mu_{\text{eff}}^2 / 3k_B$ .  $\mu_{\text{eff}}$  is the effective paramagnetic moment. The values derived are:  $\mu_{\text{eff}} = 2.46 \mu_B$ ,  $\theta_p = -18$  K and  $\chi_0 = 3.5 \times 10^{-3}$  emu/mol Oe. These values confirm the robustness of the  $\text{Ce}^{3+}$  moments and are consistent with those reported in Ref. [7] with the same  $\theta_p$  and a  $\mu_{\text{eff}} = 2.53 \mu_B$ . In the inset of Fig. 2a the high temperature range is depicted as the inverse susceptibility after subtracting  $\chi_0$ .

The field dependence of the magnetization, measured up to  $\mu_0 H = 5$  T, is displayed in Fig. 2b. Only a slight variation in the slope of  $M(H)$  is observed between 1.8 and 3 K, in agreement with the flattening of the  $\chi(T)$  dependence at low temperature. Further magnetization measurements at  $T = 1.5$  K extended up to  $\mu_0 H = 60$  T (see inset of Fig. 2b) reveal a continuous increase of  $M(H)$  with a progressive curvature approximately described by the Coqblin-Schrieffer model [11] with  $J = 1/2$  and  $T_0 = 0.8$  K as a characteristic Kondo energy scale.

## C. Electrical Resistivity

Zero-field electrical resistivity data of  $\text{CeCu}_2\text{Mg}$  and  $\text{LaCu}_2\text{Mg}$  were earlier reported for the temperature range 4–300 K revealing a tilde shape temperature dependence (in  $\rho(T)$  vs  $\log T$ ) for  $\text{CeCu}_2\text{Mg}$ , with a local maximum at about 8.5 K and a local minimum at about 80 K, and a normal metallic behavior for  $\text{LaCu}_2\text{Mg}$  [7]. In the present study, temperature and field dependent resistivity measurements,  $\rho(T, H)$ , were extended down to 0.5 K and up to 12 T. A slightly positive curvature at lowest temperatures reveals a Fermi liquid-like behavior,  $\rho(T, H) \simeq \rho_0(H) + A(H)T^2$ , below about 2 K (see Fig. 3a). The most remarkable features are a substantial reduction of the residual resistivity  $\rho_0(H)$  by about 30% when increasing the magnetic field from zero to 8 T,  $\rho_0(0 \text{ T}) = 27.3 \mu\Omega\text{cm}$  and  $\rho_0(8 \text{ T}) = 21.1 \mu\Omega\text{cm}$ , and a non-monotonic but weak variation of the  $T^2$ -coefficient  $A(H)$  which is  $0.85 \mu\Omega\text{cm K}^{-2}$  at zero field,  $1.05 \mu\Omega\text{cm K}^{-2}$  at 4 T and  $0.86 \mu\Omega\text{cm K}^{-2}$  at 8 T. The latter relates to the field dependence of the magneto-resistivity depicted in Fig. 3b which displays a structured, double vaulting field dependence of the magneto-resistivity at temperatures below 2 K.

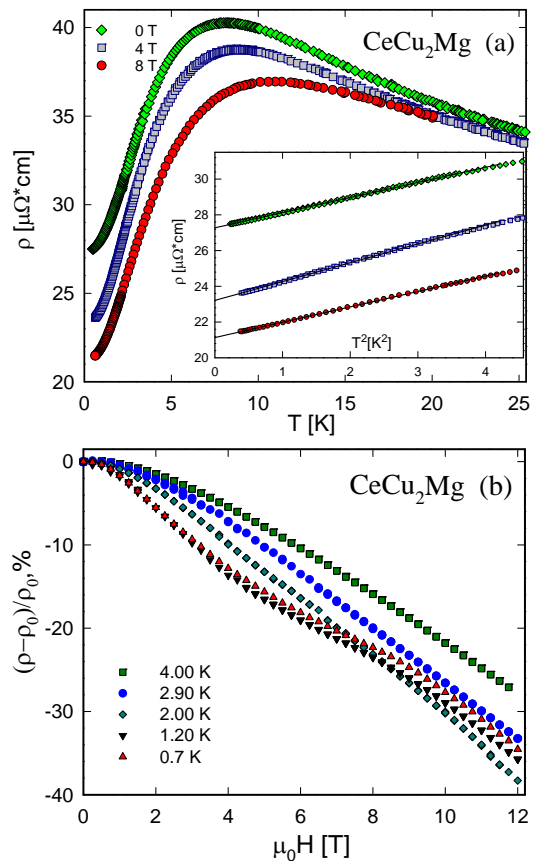


FIG. 3. (Color online) (a) Thermal dependence of the electrical resistivity,  $\rho(T)$ , measured at various external fields as labeled. Inset: corresponding  $\rho(T)$  vs  $T^2$  dependence. (b) Field dependent, relative isothermal magneto-resistivity  $[\rho(H) - \rho(H = 0)]/\rho(H = 0)$  measured at various temperatures as labeled.

The initial decrease of the magneto-resistance (compare Fig. 3b) corresponds with a typical behavior of Kondo systems, where magnetic fluctuations of the system become suppressed by increasing magnetic fields; as a consequence, the resistivity decreases. This holds in the entire temperature range studied. For the lowest temperature runs ( $T < 2$  K), a magnetic field of about 5 T induces a distinct change of  $\Delta\rho/\rho$ . This, likely, is associated with changes in the nature of the paramagnetic ground state (see discussion in section IV C).

At higher temperature,  $\rho(T)$  exhibits a maximum at  $T_{\text{max}}^\rho \approx 8.5$  K, see Fig. 3a. In general, such maxima are a characteristic of a Kondo lattice, with  $T_K \propto T_{\text{max}}^\rho$ ; below that temperature the resistivity drops due to onset of coherence among the Kondo scattering centers. Since, however, heat capacity data (see below) refer to a rather small separation of the first excited CEF level from the ground state,  $T_{\text{max}}^\rho$  is certainly influenced by crystalline electric field effects.

The low value of  $T_{\text{max}}^\rho$  obtained for  $\text{CeCu}_2\text{Mg}$ , compared with other  $\rho(T)$  maxima in Ce compounds, sug-

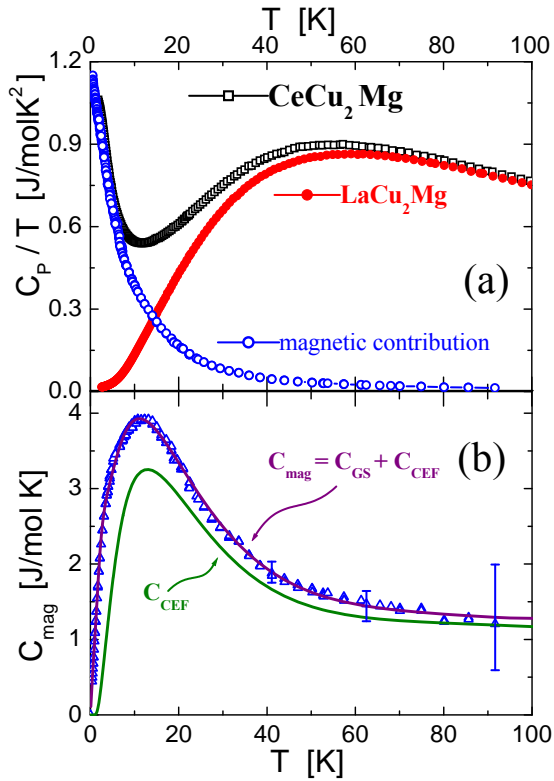


FIG. 4. (Color online) (a) High temperature specific heat up to 130 K, showing the total contribution,  $C_P/T$ , compared with the LaCu<sub>2</sub>Mg reference for phonon subtraction to obtain the magnetic contribution  $C_{\text{mag}}/T$ . (b) Analysis of  $C_{\text{CEF}}$ , the CEF Schottky contribution to the total magnetic contribution  $C_{\text{mag}}$ , using a set of Schottky anomalies (see text).

gests a relatively weak CEF effect with comparable hybridization strength in the lower and GS levels, i.e.  $\Delta_1 \approx T_K$ . Applied magnetic fields up to  $\mu_0 H = 8 \text{ T}$  decrease the maximum moderately and cause an upward shift of  $T_{\text{max}}^\rho(H)$ , roughly proportional to  $H^2$  (not shown). Above  $T_{\text{max}}^\rho(H)$ , the typical  $\rho(T) \propto -\ln T$  behavior due to Kondo scattering is progressively softened.

#### D. Specific Heat

Temperature dependent specific heat measurements, performed up to 100 K, are presented in Fig. 4a. The magnetic contribution,  $C_{\text{mag}}/T$ , is obtained by subtracting phonon and  $[6s^2 5d^1]$  band electron contributions, extracted from the isotopic compound LaCu<sub>2</sub>Mg as reported in Ref. [7], from the measured values  $C_P(T)/T$  as  $C_{\text{mag}} = C_P - C_{\text{LaCu}_2\text{Mg}}$ , see Fig. 4a.

In order to discriminate between the contributions related to the electronic degrees of freedom connected with the GS doublet and those of the excited CEF levels, the high temperature  $C_{\text{mag}}(T)$  is split as  $C_{\text{mag}} = C_{\text{GS}} + C_{\text{CEF}}$ . In absence of hybridization (i.e., the Kondo

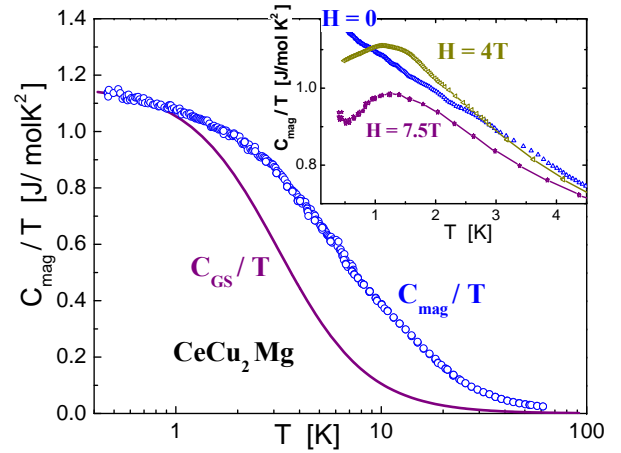


FIG. 5. (Color online) Temperature dependence of  $C_{\text{mag}}/T$  in a semi-log  $T$  representation; solid line: ground state contribution  $C_{\text{GS}}/T$  computed by subtracting the  $C_{\text{CEF}}/T$  from  $C_{\text{mag}}/T$ . Inset: effect of applied magnetic fields upon  $C_{\text{mag}}/T$  vs  $T$  at low temperature.

effect),  $C_{\text{CEF}}$  is properly described by a simple Schottky anomaly [12] because the respective levels are Dirac  $\delta$ -functions in energy. Taking into account that the CEF splits the six fold Hund's rule state (for the  $J = 5/2$  total angular momentum of  $\text{Ce}^{3+}$ ) into three Kramer's doublets with respective energies:  $\Delta_1$  and  $\Delta_2$ , at least two Schottky anomalies are expected to contribute to  $C_{\text{CEF}}$ . However, due to hybridization effects a standard Schottky anomaly cannot describe the  $C_{\text{CEF}}(T)$  dependence properly because of the level broadening due to Kondo interactions.

To take into account that effect, the excited CEF levels are computed as a sum of levels, symmetrically distributed in energy around the nominal values  $\Delta_1$  and  $\Delta_2$  [13]. This simplified description mimics the broadening ( $\delta_i \propto |n(E_F)J_K|^2 T$  [14]) of each doublet centered at  $\Delta_i$ . The formula applied reads:

$$C_{\text{CEF}}(T) = \sum_i \sum_{j=-1,0,1} A_{i,j} \left[ \frac{\left( \frac{\Delta_i + j \cdot \delta_i}{2T} \right)}{\cosh \left( \frac{\Delta_i + j \cdot \delta_i}{2T} \right)} \right]^2 \quad (2)$$

where  $A_{i,j} = R\lambda_i a_{i,j}$  and  $R$  is the gas constant. The degeneracy ratio  $\lambda_i$  between the states involved decrease, i.e.  $\lambda_1 = 1$  and  $\lambda_2 = 1/2$ . The coefficients  $a_{i,j}$  account for the weight of each level centered at the respective energies  $\Delta_i$ . For this fit, we used a set of levels composed by a central doublet with weights  $a_{i,0} = 1/2$  and two singlets with  $a_{i,\pm 1} = 1/4$  which are located at  $\Delta_i \pm \delta_i$ . The Kondo broadening  $\delta_i$  can further be seen as a measure for the error bar of the obtained CEF levels  $\Delta_i$ .

The result of this fit to the  $C_{\text{mag}}(T)$  data is shown in Fig. 4b, with the parameters for the  $C_{\text{CEF}}(T)$  contribution,  $\Delta_1 \approx 24 \text{ K}$  and  $\Delta_2 \sim 200 \text{ K}$ , and the respective effective broadening,  $\delta_1 = 15 \text{ K}$  and  $\delta_2 \sim 140 \text{ K}$ . The

rather low value of  $\Delta_1$  is confirmed by the peculiar behavior of this compound discussed in the next section. The significance of the given value of  $\Delta_2$  is, however, weak. Nevertheless, this scheme satisfies the correct overall entropy gain. Since  $C_{\text{mag}}(T)$  contains  $C_{\text{GS}}$  and  $C_{\text{CEF}}$ , and Eqn. (2) only accounts for the latter, the pure  $C_{\text{GS}}$  contribution (included in Fig. 4b) is obtained as the difference between the two curves at low temperature, i.e.  $C_{\text{GS}} = C_{\text{mag}} - C_{\text{CEF}}$ .

Figure 5 displays a semi-logarithmic representation of  $C_{\text{mag}}/T$ . A monotonic decrease for more than two decades in temperature is observed starting from the heavy fermion value of  $C_{\text{mag}}(T \rightarrow 0)/T \approx 1.2 \text{ J/molK}^2$ . The flattening of  $C_{\text{mag}}(T)/T$  vs  $\log(T)$  occurs at a similar temperature range as for  $M(T)/H$  shown in Fig. 2a. This suggests that both parameters depend on the same mechanism governing the GS behavior which will be discussed in the next Section.

## IV. DISCUSSION

### A. Low temperature properties

To gain insight into the magnetic nature of the GS, we have performed specific heat measurements under magnetic fields of  $\mu_0 H = 4$  and 7.5 T. An incipient anomaly emerges for  $\mu_0 H = 4$  T slightly above 1 K. This anomaly is much better defined for  $\mu_0 H = 7.5$  T as it can be observed in the inset of Fig. 5 in comparison to the zero field data. The emergence of this anomaly indicates that  $\text{Ce}^{3+}$  magnetic moments are progressively polarized by magnetic fields. Notably, magnetic field effects are much weaker than those reported for typical HF whose GS are affected by the Kondo effect. For comparison, one may refer to exemplary HF compounds like  $\text{CeCu}_{5.9}\text{Au}_{0.1}$  [15] and  $\text{CePd}_{0.15}\text{Rh}_{0.85}$  [16]. These two systems were especially selected because they show similar values of  $C_{\text{mag}}/T$  at  $T \approx 1$  K as  $\text{CeCu}_2\text{Mg}$ , and their behaviors can be compared under a similar magnetic field of  $\mu_0 H = 4$  T. In both selected cases  $C_{\text{mag}}/T$  decreases by more than 50% under a field of 4 T as compared to the zero-field values. On the contrary, in  $\text{CeCu}_2\text{Mg}$  the maximum of the anomaly first exceeds the zero field specific heat and then decreases for 7.5 T. Moreover, no shift occurs in temperature of the anomaly even under  $\mu_0 H = 7.5$  T, in clear contrast to both mentioned HF compounds.

Such different behaviors evidence that in the two HF compounds  $\text{CeCu}_{5.9}\text{Au}_{0.1}$  and  $\text{CePd}_{0.15}\text{Rh}_{0.85}$  magnetic interactions are weakened by the Kondo screening acting on the localized magnetic moments, whereas in  $\text{CeCu}_2\text{Mg}$  the robust (non-screened) magnetic moments simply point on random directions due to the effect of magnetic frustration. Similar behavior occurs in the spinice compound  $\text{Dy}_2\text{Ti}_2\text{O}_7$  [17]: here an applied magnetic field relieves that frustration by progressively aligning the moments along the field direction.

The symmetry of Ce atomic sites in  $\text{CeCu}_2\text{Mg}$  pro-

vides conditions for geometric frustration because the six Ce first magnetic neighbors (at a distance of 4.657 Å) are distributed on the hexagonal lattice [18] of the  $\text{GdPt}_2\text{Sn}$  type structure, whereas the inter-plane distance is 5.094 Å. A characteristic of magnetically frustrated systems is the strong increase of the density of low energy excitations  $\propto C_{\text{mag}}/T$  because magnetic correlations try to develop magnetic order as  $T \rightarrow 0$ , whereas frustration inhibits that possibility impeding magnetic moments alignment.

Based on the magnetic character of these excitations, one may test whether both thermal ( $C_{\text{mag}}/T$ ) and magnetic ( $\chi$ ) parameters are dominated by the same type of excitations of quasi-particles with enhanced  $m_{\text{eff}}$  which form coherent narrow bands in a periodic Ce-lattice. For such a test, the  $\chi(T)/\gamma(T)$  ratio with  $\gamma(T) = C_{\text{mag}}(T)/T$  can be computed and compared with the Wilson-ratio  $R_W = 3\mu_B^2/(\pi^2 k_B^2) = 0.014 \text{ emu K}^2/\text{J}$  [19], which strictly applies to a FL doublet ground state with  $\mu_s = 1\mu_B$  and in the limit  $\mu_0 H \rightarrow 0$ . The  $R_W$  ratio extracted for this compound:  $\chi/\gamma|_{T \rightarrow 0} = 0.042 \text{ emu K}^2/\text{J}$  (see the inset of Fig. 6) is larger than that of other well known HF Ce-compounds like  $\text{CeCu}_6$ :  $0.020 \text{ emu K}^2/\text{J}$ ,  $\text{CeAl}_3$ :  $0.030 \text{ emu K}^2/\text{J}$ , and  $\text{CeCu}_2\text{Si}_2$ :  $0.018 \text{ emu K}^2/\text{J}$  [20]. The increase of this ratio at  $T \geq 3$  K indicates that the first excited CEF level starts to contribute with a different ratio between its magnetic and thermal components. These features are corroborated by the low temperature  $\rho = AT^2$  dependence of the electrical resistivity.

The zero-field value of the Kadowaki-Woods (KW) ratio of  $\text{CeCu}_2\text{Mg}$ ,  $A/\gamma^2 \simeq 0.64 \times 10^{-6} \mu\Omega\text{cm}(\text{molK/mJ})^2$ , is significantly smaller than that of systems like  $\text{CeCu}_6$  with  $A/\gamma^2 \sim 10^{-5} \mu\Omega\text{cm}(\text{molK/mJ})^2$  [21, 22]. Due to the effect of the external magnetic field on  $C_{\text{mag}}$ , however, the KW ratio of  $\text{CeCu}_2\text{Mg}$  increases almost by a factor of two reaching  $A/\gamma^2 \simeq 1.1 \times 10^{-6} \mu\Omega\text{cm}(\text{molK/mJ})^2$  at 8 T.

### B. High temperature properties

The magnetic contribution to the entropy,  $S_{\text{mag}}(T)$ , follows from  $S_{\text{mag}} = \int (C_{\text{mag}}/T) dT$ . As shown in Fig. 6 the entropy gain reaches about 87% of the total expected entropy ( $R \ln 6$ ) at 100 K. However, an extrapolation of the entropy, using the fit of the specific heat presented in Fig. 4b, collects more than 95% of the total value (continuous curve in Fig. 6).

The monotonic decrease of  $C_{\text{mag}}(T)/T$  with temperature in Fig. 4b indicates that the CEF excited levels are affected by a hybridization broadening comparable to their respective  $\Delta_i$  splitting. Since these parameters are obtained using a series of Schottky anomalies with a distribution of  $\delta$ -Dirac type levels, the actual  $T_{K_i}$  values are expected to be a little larger because  $C_{\text{CEF}}(T \rightarrow 0) \propto \exp(-\Delta/T)$ , whereas for a Kondo anomaly one expects to have  $C_K(T \rightarrow 0) \propto T$ . In any case, the extracted splitting of the first CEF level is no-



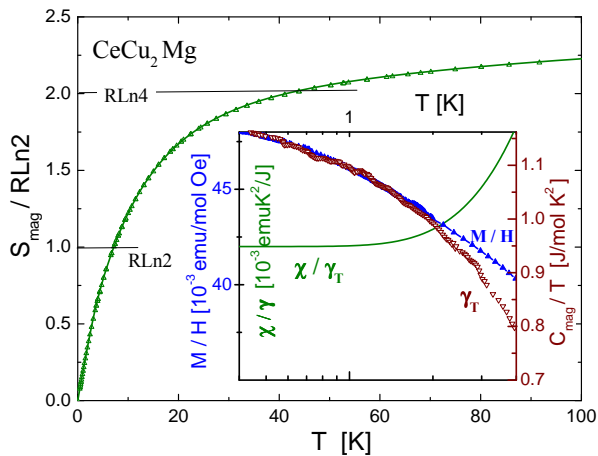


FIG. 6. (Color online) Thermal increase of the entropy normalized to the entropy of a doublet (i.e.  $R \ln 2$ ). The continuous curve is the entropy evaluation from the fit of the specific heat performed in Fig. 5 that extrapolates towards  $S = R \ln 6$ . Inset: Comparison of low temperature  $M/H \equiv \chi$  (outer left axis) and  $C_{\text{mag}}(T)/T = \gamma_T$  (right axis). The continuous curve indicates the Wilson-like ratio for the low temperature range (inner left axis).

tably low compared to other Ce intermetallic systems. To our knowledge, similar low values of  $\Delta_i$  are only found in  $\text{CeZn}_{11}$  [23, 24] and  $\text{CeCd}_{11}$  [25], the former showing AF ordering at  $T \approx 2$  K and the latter is without magnetic order down to  $\approx 1.5$  K. The resemblance between their CEF splittings with those of  $\text{CeCu}_2\text{Mg}$  is reflected in a similar  $C_{4f}(T)$  dependence at high temperature. However, in the case of  $\text{CeCu}_2\text{Mg}$  a slightly larger scale of  $T_{K_i}$  favors the energy overlap between the excited levels. The constant value of  $\chi/\gamma_T$  up to  $T \approx 2$  K allows to estimate a lower limit of the first CEF excited level contribution. In  $\text{CeZn}_{11}$  and  $\text{CeCd}_{11}$ , the low CEF overall splitting is explained by the almost isotropic electronic cage of Ce neighboring atoms [25]: Zn-[ $4s^2$ ] and Cd-[ $5s^2$ ]. This scenario also applies to  $\text{CeCu}_2\text{Mg}$  because of the respective Cu-[ $4s^1$ ] and Mg-[ $3s^2$ ] electronic character of the ligand atoms. Notice that this compound is a peculiar case among Ce-ternaries because both Ce-ligands have pure  $s$ -electronic configurations in contrast to the usual  $p$  or  $d$  character of some ligands.

### C. Frustration and Fermi Liquid coexistence

The low temperature properties of  $\text{CeCu}_2\text{Mg}$  show some peculiar features that can be understood in the frame of the coexistence of two phenomena. Starting with the  $\rho(T, H)$  dependence, one can see from Fig. 3a that, while magnetic field induces a decrease of  $\rho_0(H)$ , the  $\rho = AT^2$  dependence is only slightly affected. This behavior indicates that some type of magnetic disorder is progressively reduced, whereas the coherent character

remains unchanged.

Coincidentally,  $C_{\text{mag}}(T)$  shows a decrease of the intensity of the anomaly centered at  $T_{\text{max}} \approx 1.2$  K independently of the applied field (see inset of Fig. 5), whereas a FL signature provided by the Wilson and KW ratios appears at the same range of temperature (see inset of Fig. 6). The decrease of  $C_{\text{mag}}/T$  at  $T_{\text{max}}$  suggests a transfer of degrees of freedom from one subsection in the phase space of excitations, i.e. from frustrated spin-liquid-like excitations (see Ref. [26]) essentially contributing to  $\rho_0$ , to another subsection, i.e. Kondo FL-type excitations. The difference in the nature of these excitations does not seem to be that of distinctly different phases separated by a broken symmetry because  $\rho(T, H)$  does not behave like in a parallel circuit rather as in a series one. Otherwise, the FL component  $\rho_{\text{FL}} = AT^2$  would short-circuit the frustrated one. This suggests that the coexistence of frustrated RKKY and Kondo interactions is an intrinsic property of the system.

All these features converge in the framework proposed by Coleman and Nevidomskyy [27] where the interplay between frustrated (Q) and Kondo (K) components allows to discuss the physics of HF in a broader perspective. Contrary to the simple picture that these mechanisms exclude each other, the combined 'Q-K' phase diagram shows that a spin liquid, which carries a degree of frustration able to inhibit the formation of magnetic order, may transform into a heavy FL by the increase of the K strength.

Applying these concepts to the present study, one may locate  $\text{CeCu}_2\text{Mg}$  into the intermediate regime in-between a paramagnetic spin liquid (or valence bond metal) phase and a paramagnetic heavy Fermi liquid phase (see Ref. [27]). This possibility is supported by the fact that the magnetic field is able to drive the system in the heavy-FL direction, without changing the Q value significantly as reflected in the  $T_{\text{max}} \neq f(H)$  character, but inducing a progressive transfer of degrees of freedom revealed by the reduction of  $\rho_0$  and by a marked increase of the Kadowaki-Woods ratio.

## V. CONCLUSIONS

$\text{CeCu}_2\text{Mg}$  was re-investigated by performing lower temperature transport and thermal measurements complemented with a detailed analysis of the high temperature results. Altogether these data allowed us to shed more light on the peculiar behavior of this compound. The lack of magnetic order is confirmed down to 0.4 K, occurring despite of the robustness of Ce magnetic moments. The relatively low energy scale of Kondo interaction of the ground state is reflected in the enhanced  $C_{\text{mag}}/T|_{T \rightarrow 0}$  of this heavy fermion compound that grows up to almost  $1.2 \text{ J/mol K}^2$ . The lack of magnetic order is attributed to frustration of magnetic interactions in a hexagonal structure of the magnetic atoms in the plane. This scenario is supported by a specific heat anomaly

induced by applied magnetic fields around 1.2 K that decreases in intensity without changing its position in temperature. A small CEF lower level splitting,  $\Delta_1 \approx 24$  K, characterizes this compound. Furthermore, it exhibits a comparable Kondo broadening of this level,  $\delta_1 \approx 15$  K, that contributes to the physical properties down to quite low temperature.

The temperature dependent electrical resistivity displays a maximum at around 8 K, before entering a coherent state at lower temperature which does not change significantly under magnetic field. While this characteristic for a FL behavior is almost not affected by magnetic field, the residual resistivity decreases by about 30% between 0 and 8 T.

This feature, together with the specific heat behavior

under magnetic field, reveal an outstanding characteristic of this compound as a possible experimental example for a system tuned into an intermediate paramagnetic region of the frustration-Kondo phase diagram for heavy fermion materials proposed in Ref. [27].

## ACKNOWLEDGMENTS

We acknowledge the support of the HLD-HZDR, member of the European Magnetic Field Laboratory (EMFL). L.S. acknowledges an Ernst Mach stipend from the ÖAD.

† Gerfried Hilscher deceased on May 28<sup>th</sup> 2016, during finalization of the manuscript.

- 
- [1] P. W. Anderson, *Phys. Rev.* **124**, 41 (1961).  
 [2] G. R. Stewart, *Rev. Mod. Phys.* **73**, 797 (2001).  
 [3] P. Schlottmann and P. Sacramento, *Advances in Physics* **42**, 641 (1993).  
 [4] S. Doniach, *Physica B+C* **91**, 231 (1977).  
 [5] M. Lavagna, C. Lacroix, and M. Cyrot, *Physics Letters A* **90**, 210 (1982).  
 [6] J. G. Sereni, *Journal of Low Temperature Physics* **179**, 126 (2015).  
 [7] M. Giovannini, E. Bauer, G. Hilscher, R. Lackner, H. Michor, and A. Saccone, *Physica B: Condensed Matter* **378–380**, 831 (2006).  
 [8] J. G. Sereni, in *Handbook on the Physics and Chemistry of Rare Earths*, Vol. 15, edited by K. A. Gschneidner Jr. and L. Eyring (Elsevier, 1991) pp. 1–59.  
 [9] Y. Skourski, M. D. Kuz'min, K. P. Skokov, A. V. Andreev, and J. Wosnitza, *Phys. Rev. B* **83**, 214420 (2011).  
 [10] B. Heying, U. Rodewald, W. Hermes, and R. Pöttgen, *Zeitschrift für Naturforschung B* **64**, 170 (2014).  
 [11] A. Hewson and J. Rasul, *Journal of Physics C: Solid State Physics* **16**, 6799 (1983).  
 [12] J. Sereni, in *Reference Module in Materials Science and Materials Engineering* (Elsevier, 2016).  
 [13] J. G. Sereni, P. Pedrazzini, M. Gómez Berisso, A. Chacoma, S. Encina, T. Gruner, N. Caroca-Canales, and C. Geibel, *Phys. Rev. B* **91**, 174408 (2015).  
 [14] L. C. Lopes and B. Coqblin, *Phys. Rev. B* **38**, 6807 (1988).  
 [15] H. v. Löhneysen, T. Pietrus, G. Portisch, H. G. Schlager, A. Schröder, M. Sieck, and T. Trappmann, *Phys. Rev. Lett.* **72**, 3262 (1994).  
 [16] J. Sereni, T. Radu, and A. Pikul, *J. Optoelectr. Adv. Mater* **10**, 1645 (2008).  
 [17] Z. Hiroi, K. Matsuhira, and M. Ogata, *Journal of the Physical Society of Japan* **72**, 3045 (2003).  
 [18] A. P. Ramirez, *Annual Review of Materials Science* **24**, 453 (1994).  
 [19] Z. Fisk, H. R. Ott, T. M. Rice, and J. L. Smith, *Nature* **320**, 124 (1986).  
 [20] A. Amato, D. Jaccard, J. Flouquet, F. Lapiere, J. L. Tholence, R. A. Fisher, S. E. Lacy, J. A. Olsen, and N. E. Phillips, *Journal of Low Temperature Physics* **68**, 371 (1987).  
 [21] K. Kadowaki and S. Woods, *Solid State Communications* **58**, 507 (1986).  
 [22] H. Ott, H. Rudigier, Z. Fisk, J. Willis, and G. Stewart, *Solid State Communications* **53**, 235 (1985).  
 [23] Y. Nakazawa, M. Ishikawa, S. Noguchi, and K. Okuda, *Journal of the Physical Society of Japan* **62**, 3003 (1993).  
 [24] H. Hodovanets, S. L. Bud'ko, X. Lin, V. Taufour, M. G. Kim, D. K. Pratt, A. Kreyssig, and P. C. Canfield, *Phys. Rev. B* **88**, 054410 (2013).  
 [25] J. Tang and K. G. Jr., *Journal of Magnetism and Magnetic Materials* **75**, 355 (1988).  
 [26] P. W. Anderson, *Materials Research Bulletin* **8**, 153 (1973).  
 [27] P. Coleman and A. H. Nevidomskyy, *Journal of Low Temperature Physics* **161**, 182 (2010).